Resveratrol Nanoparticles enhance neuroprotective efficacy in a multiple sclerosis model

OR

Nanoparticles improve solubility of resveratrol and lead to enhanced neuroprotective effects at lower concentrations in a model of multiple sclerosis

Authors: Ehtesham Shamsher[1,6], Reas S. Khan[2], Benjamin M. Davis[1], Kimberly Dine[2], Vy Luong[1], Satyanarayana Somavarapu[3], M. Francesca Cordeiro[1,4,5*], Kenneth S. Shindler[2*]

1. Institute of Ophthalmology, University College London, London, United Kingdom.
2. Scheie Eye Institute, University of Pennsylvania, Philadelphia, United States
3. School of pharmacy, University College London, London, United Kingdom.
4. Imperial College London Ophthalmology Research Group, London, United Kingdom.
5. Western Eye Hospital, London, United Kingdom.
6. Jules-Gonin Eye Hospital, Lausanne University, Lausanne, Switzerland

*Corresponding authors

Purpose: Resveratrol is a natural polyphenol which may be useful for treating neurodegenerative diseases such as multiple sclerosis (MS) because of its antioxidant and anti-apoptotic properties. However, resveratrol's low solubility in water and low bioavailability limit its use. To date, current immunomodulatory treatments for MS aim to reduce inflammation with limited effects on the neurodegenerative component of this disease. The purpose of the current studies is to develop a novel nanoparticle formulation of resveratrol to increase its solubility, and to assess its ability to prevent optic nerve and spinal cord degeneration in an experimental autoimmune encephalomyelitis (EAE) mouse model of MS.

Methods: Resveratrol nanoparticles (RNs) were made with TPGS and Solutol using a thin rehydration technique. They were assessed for stability and encapsulation efficiency over time. EAE mice received a daily oral administration of vehicle, RNs or unconjugated resveratrol for one month. They were assessed daily for clinical signs of paralysis and weekly for their visual acuity with optokinetic responses (OKR). After one month, they were sacrificed. Their spinal cords and optic nerves were stained for inflammation and demyelination. Retinal ganglion cells were immunostained,

Results: RNs were stable for three months. The administration of RNs did not have any effect on clinical manifestation of EAE and did not preserve OKR scores. It did not reduce inflammation and demyelination in the spinal cord and the optic nerve. However, RNs were able to decrease RGC loss compared to the vehicle.

Conclusions: These promising results demonstrate that resveratrol can be formulated into stable nanoparticles which are neuroprotective by reducing RGC loss. However, these results did not show any reduction of inflammation or demyelination.

1. Introduction

Multiple sclerosis (MS) is an inflammatory and neurodegenerative disease affecting the central nervous system (CNS). The most common presenting manifestation of the disease is optic neuritis (1). To characterize the disease, well-established animal models are used. One widely used model is the experimental autoimmune encephalomyelitis (EAE) mouse model. Present treatments seek to reduce the inflammatory component of this disease with disease-modifying drugs such as interferons, glatiramer acetate, and teriflunomide, with limited effects on neurodegeneration (1). Neurodegenerative processes in MS are very important as they are responsible for disabilities including vision loss resulting in a big economic burden for our society (2).

Resveratrol is a natural polyphenol found in red wine and dark chocolate with well-documented antioxidant, anti-apoptotic and anti-inflammatory activity (3). The efficacy of resveratrol in the treatment of neurodegenerative disease models including glaucoma and Alzheimer's disease has previously been reported (4)(5). In EAE, we have previously shown that 100 mg/kg oral resveratrol is neuroprotective by reducing retinal ganglion cell (RGC) loss (2). Despite the pre-clinical promise, translation of resveratrol therapies to the clinic has been hindered by the poor water solubility and bioavailability of this molecule (3), requiring very high doses to reach therapeutic efficacy. This is problematic as high oral dosing of resveratrol can lead to sides effects including acute kidney failure (6).

To overcome the limited solubility of resveratrol, multiple investigators have sought to formulate this molecule into nanoparticles with varying degrees of success. A common constraint of such formulations is the limited concentration of resveratrol achieved and

stability of the resulting formulation, both impeding widespread clinical uptake (7). To address these limitations, the present study describes a novel resveratrol containing nanoparticle formulation demonstrating an ideal small particle size, high solubility, long-term stability, simple and readily scalable manufacture and exceptional biocompatibility. The ability of this formulation to attenuate EAE spinal cord and optic nerve disease is also assessed.

2. Material and Methods

2.1 Preparation of resveratrol nanoparticles

Resveratrol, D-α-tocopherol polyethylene glycol 1000 succinate (TPGS) and Kolliphor HS15 (Solutol) (Figure 1A and B**Error! Reference source not found.**) were obtained at the highest purity from Sigma-Aldrich (Kent, UK). TPGS was used because of its ability to solubilise hydrophobic molecules, enhance absorption and inhibit multi-drug efflux pumps such as p-glycoprotein (8). Solutol was used because of its ability to solubilise poorly soluble molecules for oral and parenteral drug delivery (9). Resveratrol nanoparticles (RNs) were prepared using the thin rehydration technique previously described (10). Briefly, resveratrol, TPGS and Solutol were dissolved in ethanol at different concentrations (Sigma-Aldrich, Kent, UK) with heating at 37°C in a water bath for 10 minutes followed by ultrasonication until clarity. Next, resveratrol, TPGS and Solutol were aliquoted in a round bottom flask. Ethanol was removed by rotary evaporation (50 mmHg, 2 hours at 65°C) with a Rotavapor R210 with a V850 Vacuum controller (Buchi, Flawil, Switzerland) while protected from light. After evaporation for 2 hours, the thin film was rehydrated at 55°C using a buffer of 10 mM HEPES, 50 mg/ml trehalose (HT) (both obtained from Sigma-Aldrich, Kent, UK) and 0.075% sodium metabisulfite (Sigma-Aldrich, Kent, UK). Unencapsulated resveratrol

was removed with a 0.22 µm filter (33 mm Millex filter, Merck Millipore, Massachusetts, USA). RNs containing Solutol were stored at 4°C while protected from light. Each formulation was made in triplicate.

2.2 Lyophilisation of resveratrol nanoparticles

Lyophilisation of RNs was achieved by aliquoting 500 µl of RNs in 1.75 ml screw neck squat form glass vials (CamLab, Cambridge, UK) at 25°C before freezing at -60°C for 2 hours at 760 Torr. Next, primary drying was performed at -38°C and 200 mTorr for 24 hours followed by a secondary drying at 25°C and 200 mTorr for 2 hours. Immediately upon completion of secondary drying, samples were capped and stored at 25°C. For stability assessment, freeze-dried samples were rehydrated for 30 minutes in 500 µl of 0.22 µm filtered distilled water with gentle mixing and stored at 4°C.

2.3 Resveratrol loading efficiency

RN loading efficiency was determined by spectroscopic techniques using a spectrophotometer (Malvern, Massachusetts, USA). RNs were dissolved to 1:1500 in dimethyl sulfoxide (DMSO) and their absorbance measured at 328 nm wavelength normalised to empty nanoparticles (vehicle). 328 nm was determined as being the peak absorption wavelength (Figure 1A). The concentration of resveratrol in each formulation was determined using the molar extinction coefficient of resveratrol at 328 nm. It was calculated from the standard curve of resveratrol (Figure 1B) using the Beer-Lambert law:

$$\mathbf{A = \varepsilon \cdot l \cdot C}$$

As the absorbance **A** of resveratrol is proportional to its concentration **C** and extinction coefficient **Ɛ**, **Ɛ** can be determined if **A** and **C** are known. The absorbance of resveratrol at 328 nm was used here. **l** is equal to 1 cm as it is the length of the cuvette used. **Ɛ** was used in the following equation to determine the micellar drug concentration (**MDC**) of resveratrol in the formulation:

$$\mathbf{MDC\ (mg/ml) = A/Ɛ \cdot M_w \cdot DF}$$

where **A** was the absorbance of resveratrol at 328 nm, $\mathbf{M_w}$ the molecular weight of resveratrol (228.25 g/mol) and **DF** the dilution factor in DMSO (usually 1500).

Finally, the encapsulation efficiency (**EE**) of each formulation was calculated using the equation:

$$\mathbf{EE\ (\%) = 100 \cdot [R]_S/[R]_O}$$

where $\mathbf{[R]_s}$ is the concentration of resveratrol calculated spectroscopically (also called **MDC**) after filtering it through a 0.22 µm filter and $\mathbf{[R]_o}$**,** the concentration of resveratrol added originally to the formulation. Each formulation was replicated three times to assess its concentration and stability over time.

2.4 Dynamic light scattering

Particle size was measured using a Malvern Zetasizer (Massachusetts, USA) which uses the dynamic light scattering (DLS) technique based on Brownian motions (11). Measurement of particle diameter and polydispersity index (PDI) were carried out on three formulations for each experimental condition and time point. RNs were diluted 1 in 10 in the appropriate buffer. The zetasizer is able to give particle diameter because

a laser beam scattered differently through the sample due to particles' Brownian motion which induces a variability in intensity measured by a detector. The rate of intensity fluctuation is determined by the size of the particle. If the fluctuation rate is high, the particles are small, otherwise they are large. Large particles diffuse slowly whereas small particles diffuse rapidly.

2.5 Resveratrol release assays

Free resveratrol (dissolved in 95% ethanol), RNs made from TPGS and Solutol containing 10 mg/ml resveratrol were loaded into a 1 ml 3.5-5.0 kDa Spectra-Por Float-A-Lyzer dialysis cassette (Sigma-Aldrich, Kent, UK). Samples were dialysed against 200 ml of PBS (Sigma-Aldrich, Kent, UK) on a hot plate at 37°C and stirring at 50 rpm. 10% Tween-80 (Sigma-Aldrich, Kent, UK) was added to the PBS to act as a sink for released drug cargo which has poor water solubility. At specified time points, 200 µl of dialysed buffer were removed from the mixture and replaced with fresh buffer. Resveratrol concentration was calculated using methods described in section 2.3. Each experiment was carried out in triplicate. Data obtained were fit to a single-phase association:

$$\mathbf{Y = Y_0 + (Plateau - Y_0) \cdot (1 - e^{-Kx})}$$

where $\mathbf{Y_0} = 0$, **Plateau** is the maximum release and **K** is the rate of resveratrol release (h^{-1}). **K** was used to calculate the half-life ($\mathbf{t_{1/2}}$) of resveratrol release as:

$$\mathbf{t_{1/2}\ (h) = \ln(2)/K}$$

2.6 Animal handling

All animal experiments were performed in accordance with the ARVO Statement for the Use of Animals in Ophthalmic and Vision Research and with the ARRIVE guidelines. Procedures were reviewed and approved by the Institutional Animal Care and Use Committee at the University of Pennsylvania. 27 C57BL/6J 6-week-old female mice (The Jackson Laboratory, Maine, USA) weighing approximately 20 g were used. All animals were housed in an air-conditioned, 21°C environment with a 12 h light-dark cycle where food and water were available *ad libitum*.

2.7 Experimental autoimmune encephalomyelitis mouse model and clinical scoring

EAE was induced as previously described (2). Mice were anaesthetised with a solution of 0.2 ml of 10 mg/ml ketamine (Sigma, Missouri, US) and 1 mg/ml xylazine (Sigma, Missouri, US) administered intraperitoneally. They were immunised with 300 µg MOG peptide 35-55 mixed with complete Freund's adjuvant (CFA; Difco, Michigan, US) containing 2.5 mg/ml mycobacterium tuberculosis (Difco, Michigan, US) injected subcutaneously in two separate doses (150 µg each) in different areas on the back. Control mice (non-EAE control; n=5) received an equivalent volume of PBS diluted in CFA. Control and immunised mice received 200 ng pertussis toxin (List Biological, California, US) by intraperitoneal injection on the immunisation day and 2 days post-immunisation.

Mice were scored for the severity of the EAE with a clinical EAE score with a scale from 0 to 5 as previously described (2) and shown in Table 1. The scoring was carried out by a masked investigator unaware of the treatment group.

Disease manifestation	Score
Normal state	0
Tail partially paralysed	0.5
Tail fully paralysed or waddling gait	1.0
Tail partially paralysed and waddling gait	1.5
Tail fully paralysis and waddling gait	2.0
One limb partially paralysed	2.5
One limb fully paralysed	3.0
One limb fully paralysed and the other one partially	3.5
Two limbs fully paralysed	4.0
Moribund state	4.5
Death	5.0

Table 1. Clinical EAE score.

2.8 Resveratrol treatments

Freeze-dried resveratrol formulation made with TPGS/Kolliphor HS15, freeze-dried empty nanoparticles (TPGS/Kolliphor HS15 only as the vehicle) and unconjugated resveratrol suspended in PBS (RSV) were used. Freeze-dried samples were rehydrated in milli-Q® water 30 minutes before use. Mice were treated once a day for 30 days from day 1 post-immunisation by oral gavage with the vehicle equivalent to 16.9 mg/kg RNs (N=5 mice), 16.9 mg/kg RNs (N=6), 16.9 mg/kg RSV (N=5) or 100 mg/kg RSV (N=6).16.9 mg/kg RNs was used because it is the maximal amount of RNs which could be solubilised in 100 µl PBS for oral gavage. Control groups received an equivalent amount of unconjugated resveratrol and vehicle was used. 100 mg/kg RSV was used because it is the minimum oral dose that was previously demonstrated to attenuate EAE in our previous study (2).

2.9 Measurement of optokinetic response (OKR)

In order to assess the visual function, OptoMotry software and apparatus (Cerebral Mechanics Inc., Medicine Hat, Alberta, Canada) were used to measure the OKR as

previously described (12). Briefly, mice were put at the centre of a platform without movement restriction in a closed chamber comprised of four screens and a camera used to detect if they were tracking a 100% contrast grating with varying spatial frequency. The grating started at a spatial frequency of 0.042 cycles/degree and increased progressively. The highest spatial frequency at which mice were able to track correlated with their visual acuity. All data are given in cycles/degree.

2.10 Optic nerve and spinal cord inflammation and demyelination grading

Mice were transcardially perfused with 1xPBS followed by 4% paraformaldehyde (PFA). Optic nerves and spinal cords were isolated, embedded in paraffin and cut in 5 µm thick sections (longitudinally for optic nerves and transversely for spinal cords). Next, they were stained for hematoxylin and eosin (H&E) to grade the inflammatory cell infiltrate by a blinded investigator under light microscopy. Although H&E staining is not specific for macrophages, studies have shown that gross cellularity stained with H&E correlates with macrophage staining (13). Spinal cords were transected at multiple levels into 5-6 sections/mouse, and all sections from one mouse were embedded together in a single paraffin block to ensure that all levels of the spinal cord were cut and included on each slide for staining and quantification. The grading for optic nerves on the entire length of longitudinal section was performed using a 0-4 point scale previously described (14): 0= no infiltration, 1= mild cellular infiltration (focal inflammation involving less than 25% of the entire length of the optic nerve), 2= moderate infiltration (between 25% to 50% of the optic nerve involved), 3= severe infiltration (50 to 75% involved) and 4= massive infiltration (>75% involved). For spinal cords, the following 0-3 point scale was used as previously described (14) on the whole slide containing transverse sections from all spinal cord levels: 0= no inflammation, 1=

mild inflammation (less than 5 small foci of white matter inflammatory cell infiltration), 2 = moderate inflammation (5-9 small foci of inflammation or 1-2 large areas of inflammation) and 3= severe inflammation (more than 10 small foci or more than 2 large areas of inflammation).

To detect demyelination, longitudinal sections of optic nerves and transverse sections of spinal cords were stained with Luxol Fast Blue (LFB; Sigma-Aldrich, Kent, UK) and graded using a point scale previously described (14). For spinal cords, the grading was as follow: 0= no demyelination, 1= rare foci of demyelination, 2= a few areas of demyelination, and 3= large confluent areas of demyelination. For optic nerves, the grading was as follow: 0= no demyelination, 1= scattered foci of demyelination, 2= prominent foci of demyelination, and 3= large (confluent) areas of demyelination.

2.11 Quantification of retinal ganglion cell survival

Following perfusion, retinas were dissected, immunostained for Brn3a and quantified as described previously (12). They were washed and permeabilised in PBS + 0.5% Triton x-100 three times prior to freezing at -80°C for 15 min for antigen retrieval. Next, retinas were washed in PBS + 0.5% Triton x-100 before incubation at 4°C overnight with a rabbit anti-Brn3a antibody (SC-411 003, Synaptic Systems, Göttingen, Germany) diluted 1:2000 in blocking buffer (PBS, 2% BSA, 2% Triton x-100). The following morning, retinas were washed four times in 1xPBS prior to a 2-hour incubation with the donkey anti-rabbit secondary antibody (A21206, Alexa Fluor 488, Invitrogen, Paisley, US) diluted to 1:500 in the blocking buffer. Finally, retinas were washed 4 times in 1xPBS and mounted vitreous side up on slides with vectashield (Vector Laboratories,

California, US). RGCs were imaged using a fluorescence microscope at 20x magnification in 12 standard fields: 1/6, 3/6 and 5/6 from the retinal radius in each quadrant and counted by a masked investigator with ImageJ analysis software.

2.12 Statistical analysis

All data were analysed with the software GraphPad Prism 6 (La Jolla, California, USA) and statistical tests (Student's T-test, Kruskal-Wallis Test and ANOVA) were used as appropriate. All results are presented as mean ± the standard error of the mean (SEM). Results are considered statistically significant if $p<0.05$.

3. Results

3.1 Formulation of resveratrol

3.1.1 Determination of critical micelle concentration with spectroscopic methods

In order to overcome resveratrol's low solubility in water and instability in physiological solutions, it was encapsulated in micelles. As discussed above (*see 2.3)*, the concentration of resveratrol encapsulated in these micelles was assessed by spectrophotometry. First, to calculate resveratrol concentration, resveratrol's peak absorbance and molar extinction coefficient were determined. 5 µg/ml resveratrol diluted in DMSO had a peak absorbance at 328 nm (Figure 1C). Based on this wavelength, the molar extinction coefficient (Ɛ) of 31,683 ± 385.5 $L.mol^{-1}.cm^{-1}$ was calculated following Beer-Lambert's law (Figure 1D). Ɛ represents the ability of a chemical species to attenuate light at a given wavelength. Importantly, TPGS/HS15 Kolliphor nanocarriers had negligible absorbance in the absence of resveratrol at 328 nm.

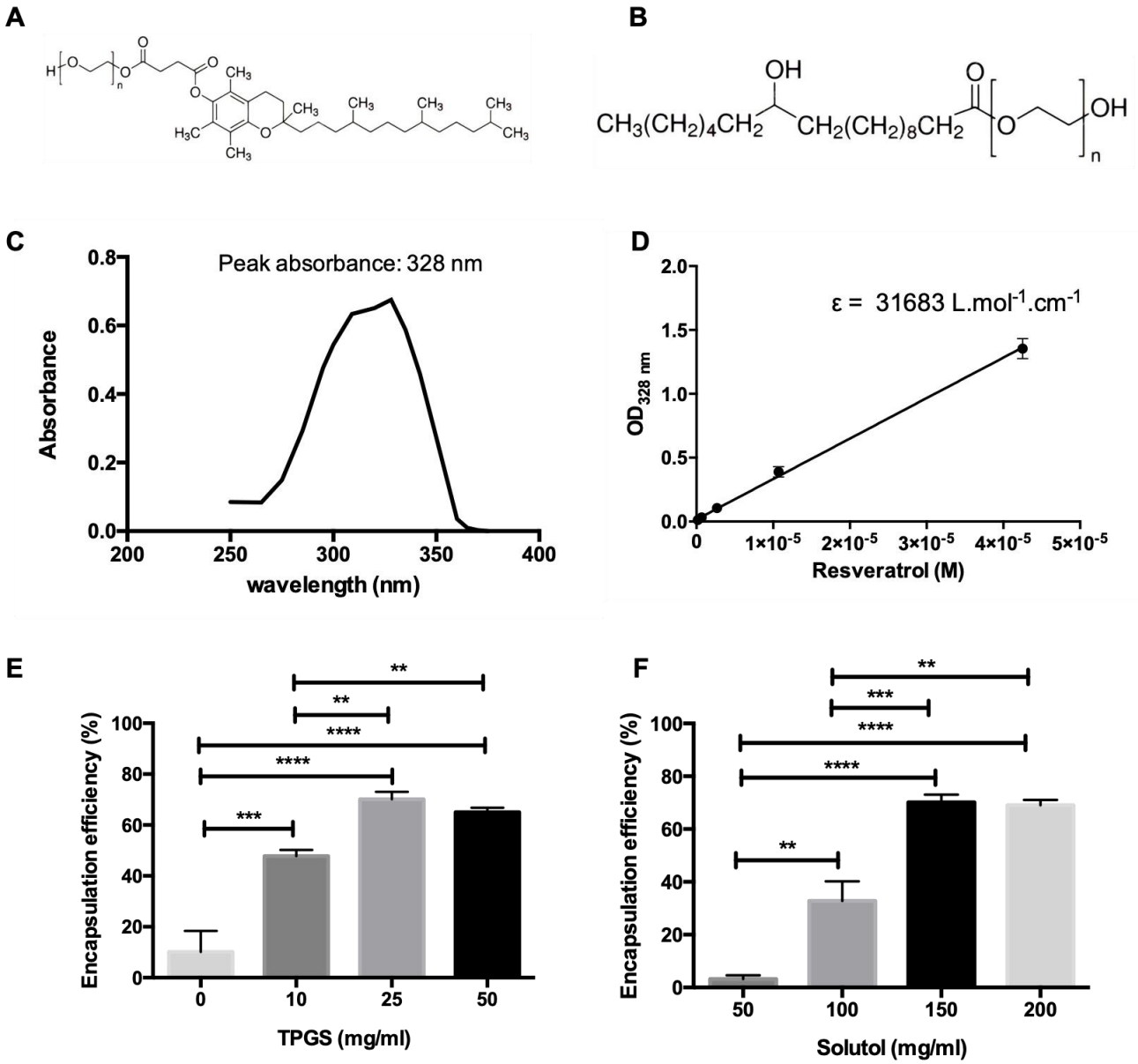

Figure 1. Spectroscopic determination of resveratrol concentration in nanoparticles. Molecular structure of **(A)** D-α-tocopherol polyethylene glycol 1000 succinate (TPGS) and **(B)** Kolliphor HS15 (Solutol). **(C)** Peak absorbance of 5 µg/ml resveratrol diluted in DMSO is at 328 nm. **(D)** Determination of the molar extinction coefficient of resveratrol in DMSO (31'683 ± 385.5 $L.mol^{-1}.cm^{-1}$). **(E)** Encapsulation efficiency of RNs containing 150 mg/ml Solutol and varying concentrations of TPGS. **(F)** Encapsulation efficiency of RNs containing 25 mg/ml TPGS and varying concentrations of Solutol. There is a significant EE difference between groups (one-way ANOVA with Tukey post-test, **p<0.01, ***p<0.001, ****p<0.0001). All results are given as mean ± SEM with N=3.

3.1.2 TPGS/Solutol HS15 nanocarriers enhance resveratrol solubility

Solutol HS15 is a polymer with no systemic toxicity and a non-ionic surfactant widely used to solubilise poorly soluble molecules for oral and parenteral drug delivery for over a decade (9). Attempts to formulate 14.22 mg/ml resveratrol using 150 mg/ml

Solutol HS15 alone achieved an encapsulation efficiency of only 10.1% ± 5.8% (Figure 1E). Addition of TPGS (from 10 to 50 mg/ml) to formulations containing 150 mg/ml Solutol improved encapsulation efficiency, with 25 and 50 mg/ml TPGS resulting in an EE of 70.1% ± 1.7% and 64.9% ± 1.0% respectively (Figure 1E). Further experiments revealed that reducing Solutol concentration below 150 mg/ml caused a substantial reduction in encapsulation efficiency (Figure 1F). As 150 mg/ml Solutol resulted in a good EE, it was used for further stability studies. This concentration of Solutol was chosen because of previously published data on Lutrol which showed that 100 mg/ml was enough to encapsulate 5 mg/ml curcumin (8).

3.1.3 Resveratrol nanoparticles are stable

The stability of resveratrol nanoparticles containing 150 or 200 mg/ml Solutol and 25 or 50 mg/ml TPGS were assessed over a period of 3 months. A summary of which is provided in Table 2. RNs comprising 50 mg/ml TPGS and 150 mg/ml Solutol were found to exhibit good stability with no decrease in EE and a constant particle size and PDI (Figure 2 A-C).

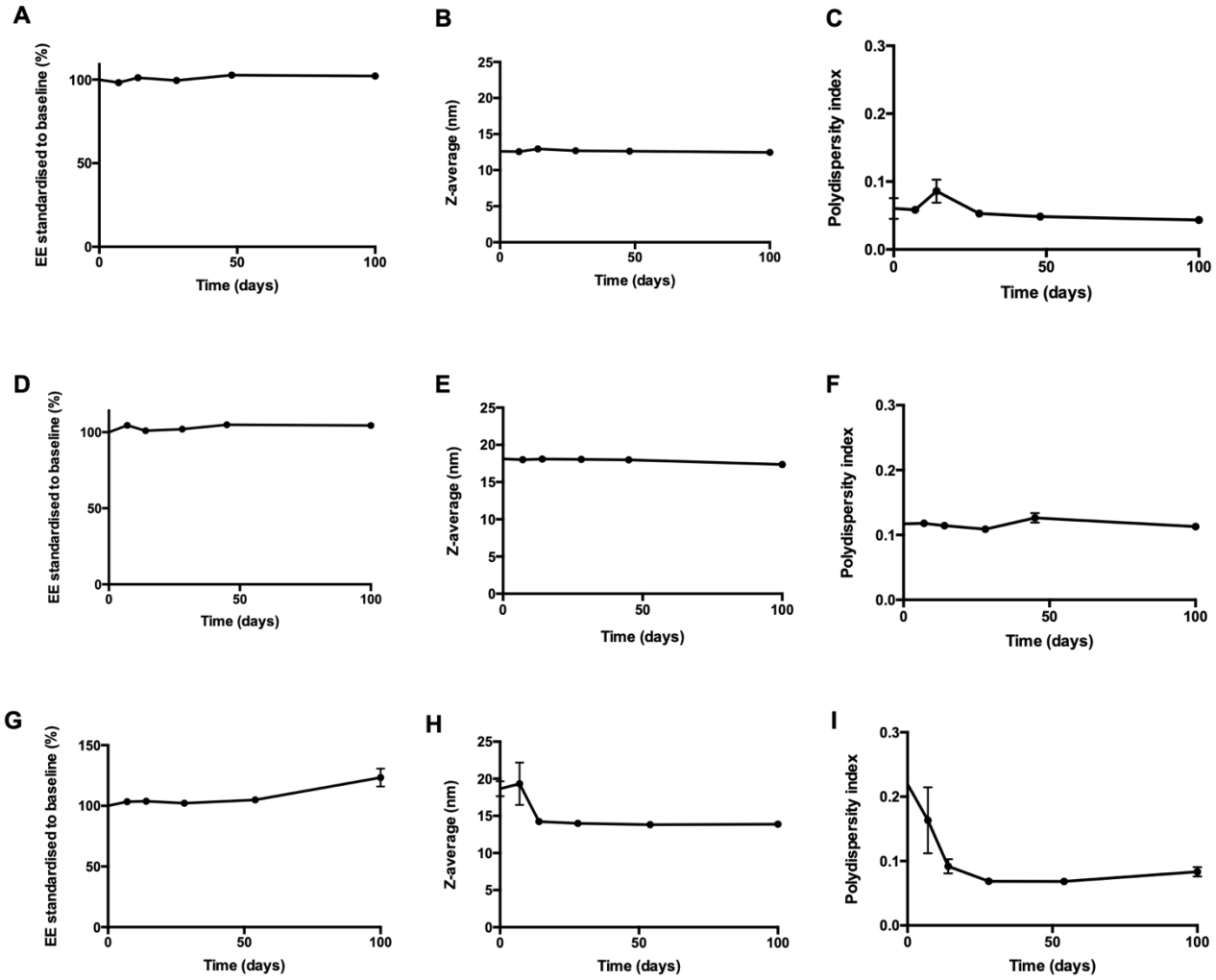

Figure 2. 14.22 mg/ml RN containing (A-C) 50 mg/ml TPGS or (D-I) 25 mg/ml TPGS and (A-F) 150 mg/ml Solutol or (G-I) 200 mg/ml Solutol stability over time. (A,D,G) The average EE standardized to baseline, **(B,E,H)** particle size and **(C,F,I)** polydispersity index were recorded in triplicate when formulations were stored at 4°C. Results are given as mean ± SEM with N=3 samples at each time point.

Similarly, RNs comprised of 25 mg/ml TPGS and 150 mg/ml Solutol or 200 mg/ml Solutol exhibited good stability with no decrease in EE and a constant particle size and PDI over 3 months (Figure 2 D-I). As both formulations exhibited comparable stability profiles, formulations containing minimal concentrations of TPGS and Solutol (25 mg/ml and 150 mg/ml respectively) were chosen for *in vivo* experiments to minimise risk of excipient toxicity.

Time	Baseline			3 months		
Characteristics	**EE (%)**	**Z-average (nm)**	**PDI**	**EE (%)**	**Z-average (nm)**	**PDI**
	50 mg/ml Solutol					
25 mg/ml TPGS	3.22 (0.81)	107.3 (73.67)	0.462 (0.132)			
	100 mg/ml Solutol					
25 mg/ml TPGS	32.79 (7.42)	24.40 (1.84)	0.145 (0.001)			
	150 mg/ml Solutol					
0 mg/ml TPGS	10.12 (5.81)	29.75 (10.77)	0.309 (0.113)			
10 mg/ml TPGS	47.78 (2.47)	23.39 (0.178)	0.126 (0.0003)			
25 mg/ml TPGS	70.12 (1.68)	18.12 (0.195)	0.117 (0.006)	73.16 (1.20)	17.36 (0.19)	0.113 (0.002)
50 mg/ml TPGS	64.92 (1.01)	12.61 (0.13)	0.060 (0.015)	66.34 (1.08)	12.47 (0.062)	0.043 (0.005)
	200 mg/ml Solutol					
25 mg/ml TPGS	69.08 (1.14)	18.67 (1.00)	0.219 (0.004)	85.36 (6.41)	13.89 (0.08)	0.083 (0.007)

Table 2. Characteristics of resveratrol nanoparticles made with TPGS and Solutol (mean ± SEM).
The formulation used for further *in vivo* studies is highlighted in orange. N=3 samples for each experimental condition.

3.1.4 Freeze-drying reduces encapsulation efficiency of RN formulations

Lyophilization of Resveratrol containing formulations was investigated as a method of further improving formulation stability (Table 2, highlighted in orange). This formulation was selected because of its highest EE and lowest concentrations of TPGS and Solutol. On rehydration with Milli-Q® ultrapure water, freeze-drying was found to result in a modest reduction of EE of 16.7% compared to not freeze-dried formulations ($p<0.01$) (Figure 3A) but retained a stable particle size (16.2±0.6 nm vs 15.2±0.5 nm, $p>0.05$) and PDI (<0.3) (Figure 3B and C) indicating the formulation remained monodisperse on rehydration (Figure 3B and C, Table 3). Figure 3D and E shows the formulation before and after freeze-drying.

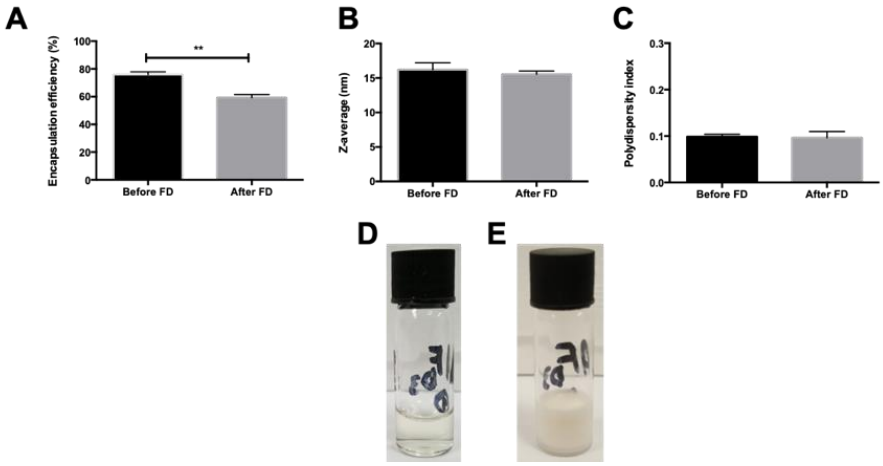

Figure 3. 14.22 mg/ml RN formulation with 25 mg/ml TPGS and 150 mg/ml Solutol before and after freeze-drying (FD). (A) Encapsulation efficiency, (B) particle size, (C) polydispersity index (unpaired Student-T test, **p<0.01). N=3 samples before and after FD. (D) Formulation before FD and (E) after.

	Before freeze-drying	After freeze-drying
Concentration (mg/ml)	10.8 (0.3)	8.44 (0.3)
EE (%)	76.0 (3.3)	59.3 (3.8)
Z-average (nm)	16.2 (0.6)	15.6 (0.5)
Polydispersity index	0.099 (0.05)	0.096 (0.007)

Table 3. Characteristics of 14.22 mg/ml RN formulation encapsulated with 25 mg/ml TPGS and 150 mg/ml Solutol before and after freeze-drying (mean ± SEM in triplicate).

The stability of these freeze-dried formulations after rehydration were assessed over 3 months. EE remained over 80% for the duration of the follow-up period (Figure 4 A). Overall, the particle size (15 nm) and PDI (<0.3) remained constant over 3 months (Figure 4 B,C). By freeze-drying RN formulations, we expect the freeze-dried formulation (before being rehydrated) to stay stable much longer than 3 months as all water content is removed and is responsible for resveratrol oxidation and hydrolysis, although this was not directly assessed in this study.

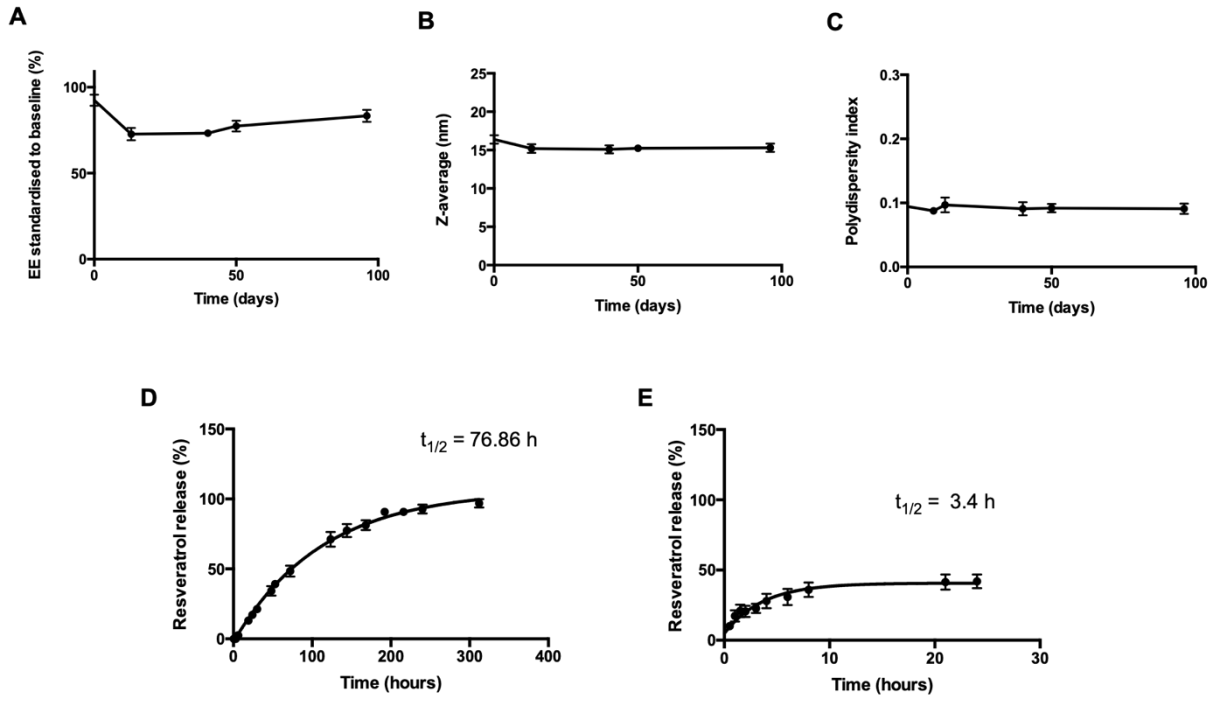

Figure 4. (A-C) Stability after rehydration of freeze-dried 14.22 mg/ml RN formulation with 25 mg/ml TPGS and 150 mg/ml Solutol. (A) The average EE standardized to baseline, **(B)** particle size and **(C)** polydispersity index were recorded when formulations were stored at 4°C. N=3 samples at each time point. **(D,E) *In vitro* release of resveratrol.** *In vitro* release of 14.22 mg/ml resveratrol from **(D)** 25 mg/ml TPGS and 150 mg/ml Solutol and **(E)** 95% ethanol in PBS at 37°C. N=3 samples assessed over time.

3.1.5 Sustained release of resveratrol nanoparticle formulations

Formulations of 14.22 mg/ml resveratrol encapsulated with 25 mg/ml TPGS and 150 mg/ml Solutol dramatically slowed the release of resveratrol compared to 14.22 mg/ml resveratrol dissolved in 95% ethanol at 37°C ($t_{1/2}$ = 76.86 h in TPGS/Solutol vs 3.4 h

in ethanol respectively, Figure 4 D,E). Less than 4% of resveratrol was released from formulated resveratrol after 6 hours whereas over 10% was released from free resveratrol in 0.5 hour. These results suggest there is limited burst release from the RN formulation, suggesting resveratrol is not merely associated with the nanoparticle surface but contained within the hydrophobic interior. This suggests the formulation may protect resveratrol from hydrolysis and has sustained release capability.

3.2 RNs prevent development of significant ascending paralysis and promote a trend toward reducing clinical manifestations of EAE

EAE mice were immunised with MOG antigen and treated daily orally from day 1 post-immunisation with vehicle, RNs or RSV for 30 days. Every day, EAE mice and sham-immunised C57BL/6J mice (non-EAE control) were graded for any clinical manifestation of ascending paralytic EAE disease. Oral administration of 16.9 mg/kg RNs, which was chosen because it was the maximum concentration of RNs achievable using oral gavage, showed a trend towards reduction in the EAE score compared to mice sham treated with an equal volume of vehicle but was not significant (1.4 ± 0.4 vs 3.0 ± 0.4 EAE score at day 30, $p>0.05$, Figure 5). Interestingly, 16.9 mg/kg RSV (concentration chosen to be the same as RNs) and 100 mg/kg RSV group (shown to be previously neuroprotective in EAE optic neuritis by Fonseca-Kelly et al. (2)) did not show the same reduction of EAE score compared to the 16.9 mg/kg RNs (2.6 ± 0.4 and 1.9 ± 0.4 vs 1.4 ± 0.4 EAE score at day 30, $p>0.05$). Notably, EAE mice treated daily with either 16.9 mg/kg RNs or 100 mg/kg RSV developed only moderate EAE disease that was not significantly different from control, non-EAE mice; whereas, EAE mice treated with saline or with 16.9 mg/kg RSV developed significantly more severe EAE ascending paralysis than control mice.

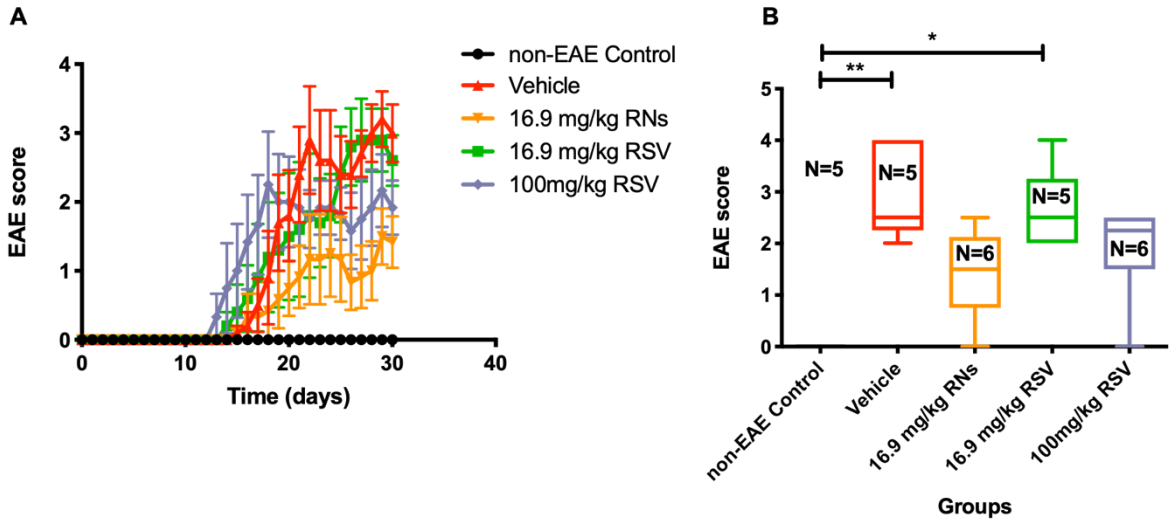

Figure 5. Clinical manifestation of ascending paralysis in EAE mice treated orally. (A) EAE score measured daily showed a strong trend toward reduced disease in the 16.9 mg/kg RNs group compared to the vehicle treated group. This trend was not significant over time as assessed by two-way repeated measures ANOVA with Tukey post-test, $p>0.05$ and EAE scores were not significantly reduced by day 30 as shown in **(B)**. Non-EAE control did not show any clinical manifestation compared to EAE mice (Kruskal-Wallis test with Dunn post-test, *$p<0.05$, **$p<0.01$**).**

3.3 RNs do not reduce spinal cord inflammation and demyelination

After one month of treatment, mice were perfused, and optic nerves and spinal cords were harvested then stained with H&E to assess inflammation and with LFB to assess demyelination. Inflammation in the spinal cord was assessed on transverse sections by masked investigators. Figure 6A-E illustrates representative areas of spinal cord demonstrating presence or absence of inflammatory cell infiltrates. Vehicle-treated EAE mice showed significant spinal cord inflammation as compared with the lack of any inflammation in control mice (0.0 ± 0.0 vs 2.4 ± 0.4, *$p<0.05$, Figure 6F). EAE mice which received 16.9 mg/kg RNs orally for three months only showed a trend towards spinal cord inflammation reduction compared to vehicle treated EAE mice, but not a significant difference (1.5 ± 0.5 vs 2.4 ± 0.4, $p>0.05$) as shown in Figure 6F. Similarly, the other groups treated with RSV did not show any significant reduction.

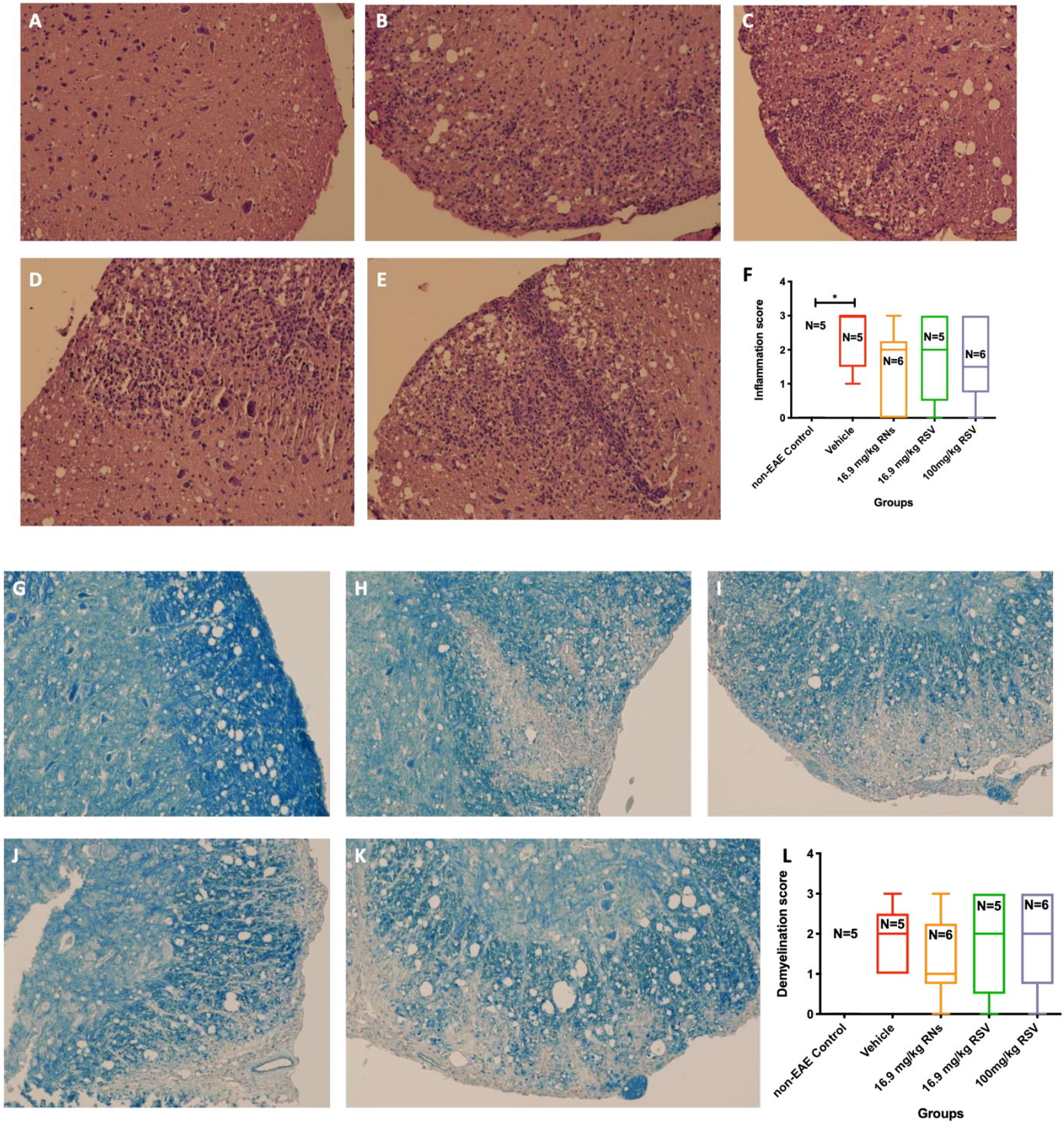

Figure 6. Spinal cord inflammation and demyelination after oral treatment with vehicle, RNs or RSV. H&E staining shows the cellularity and LFB the level of myelination in the spinal cord. Representative images of spinal cord transverse section inflammation in **(A)** non-EAE control, and EAE mice treated with **(B)** vehicle, **(C)** 16.9 mg/kg RNs, **(D)**16.9 mg/kg RSV and **(E)** 100 mg/kg RSV. **(F)** Spinal cord inflammation score was not significantly reduced with RN or RSV treatment compared to the equivalent vehicle (Kruskal-Wallis with Dunn post-test, $p>0.05$) but the vehicle had a significantly higher inflammation score than non-EAE control group (Kruskal-Wallis with Dunn post-test, *$p<0.05$). Representative images of spinal cord transverse section demyelination in **(G)** non-EAE control, and EAE mice treated with **(H)** vehicle, **(I)** 16.9 mg/kg RNs, **(J)**16.9 mg/kg RSV and **(K)** 100 mg/kg RSV. **(L)** Spinal cord demyelination score was not significantly reduced with RN or RSV treatment compared to the equivalent vehicle (Kruskal-Wallis with Dunn post-test, $p>0.05$). Images are magnified 20x.

Spinal cord demyelination was characterised by the loss of myelin stained with LFB on transverse sections of the spinal cord. Figure 6G-K illustrates representative areas of spinal cord demonstrating normal or reduced myelination. Oral administration of 16.9 mg/kg RNs resulted in a small trend towards demyelination reduction compared to vehicle, but this was not significant (1.3 ± 1.1 vs 1.8 ± 0.4, $p>0.05$) as shown in Figure 6L. RSV groups did not show any effect.

3.4 RNs reduce RGC loss

After 30 days of treatment, retinas were dissected, immunostained with a Brn3a antibody, and Brn3a+ RGCs were counted. Oral administration of 16.9 mg/kg RNs resulted in a higher RGC count than vehicle (347 ± 12 vs 202 ± 11 cells/standardised field, $p<0.0001$) as shown in Figure 7F. Importantly, 100 mg/kg RSV also achieved a higher RGC count than vehicle, similar to 16.9 mg/kg RNs (353 ± 10 vs 202 ± 11 cells/standardised field, $p<0.0001$). However, 16.9 mg/kg RSV did not show any higher RGC count compared to the vehicle (172 ± 12 vs 202 ± 11 cells/standardised field, $p>0.05$). Results suggest that RNs are neuroprotective and increase the bioavailability of resveratrol as approximately five times less concentration of RNs is needed than RSV to produce the same effect.

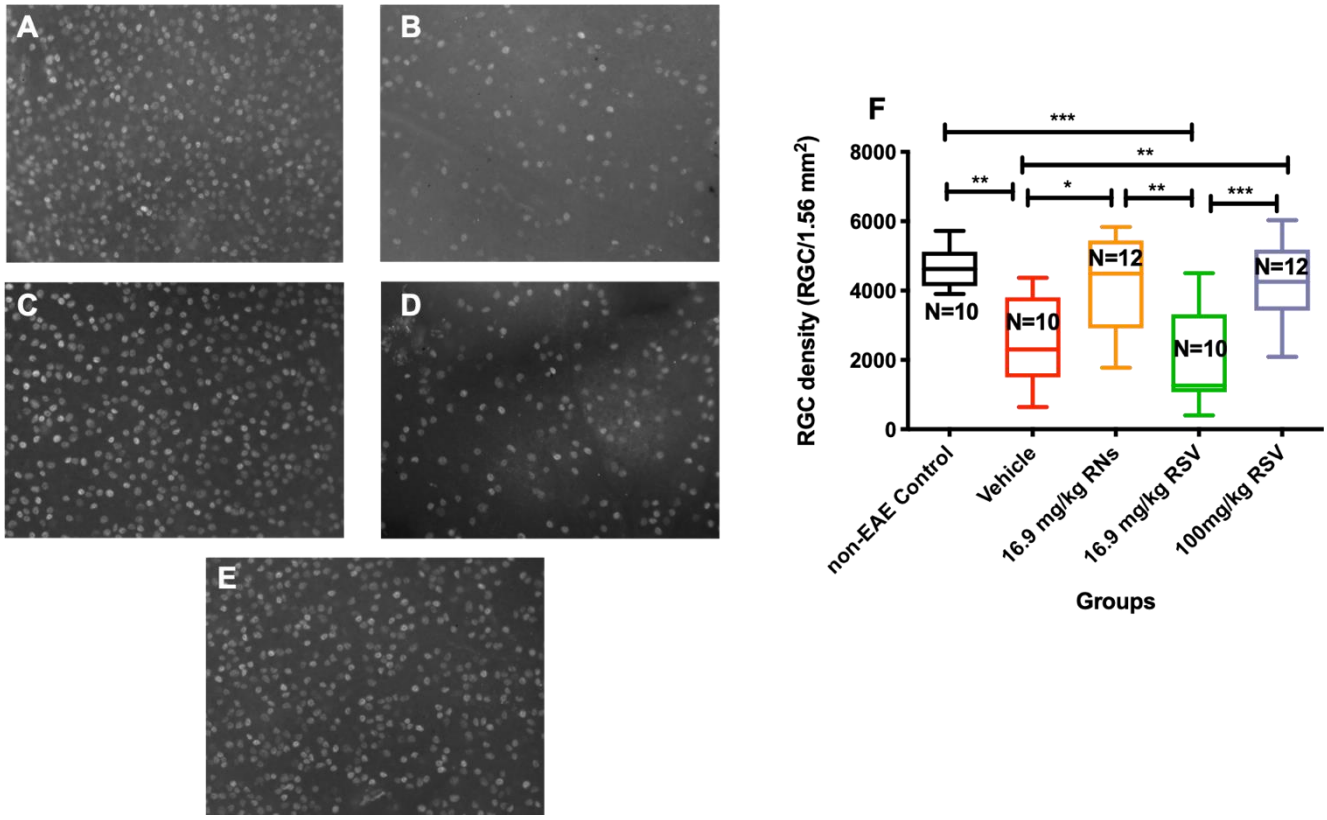

Figure 7. RGC loss after oral treatment with vehicle, RNs or RSV. Representative images of RGCs in (A) non-EAE control, and EAE mice treated with (B) vehicle, (C) 16.9 mg/kg RNs, (D)16.9 mg/kg RSV and (E) 100 mg/kg RSV. (F) RGC count was significantly increased with 16.9 mg/kg RNs and 100 mg/kg RSV treatment compared to vehicle (one-way ANOVA with Tukey post-test). Non-EAE control mice had a higher RGC count than 16.9 mg/kg vehicle and 16.9 mg/kg RSV (one-way ANOVA with Tukey post-test). Images are original magnification x20. *p<0.05, **p<0.01, ***p<0.001.

3.5 RNs do not reduce optic nerve inflammation and demyelination

Figure 8A-E shows representative H&E stained optic nerve sections used for inflammation assessment. Oral 16.9 mg/kg RNs showed a trend towards reduction of optic nerve inflammation compared to vehicle, but this was not significant (0.9 ± 0.2 vs 1.3 ± 0.3 inflammation score, p>0.05, Figure 8F). 16.9 mg/kg RSV also did not reduce inflammation. Non-EAE control mice did not show any inflammation, compared to significant inflammation present in EAE mice (p<0.05).

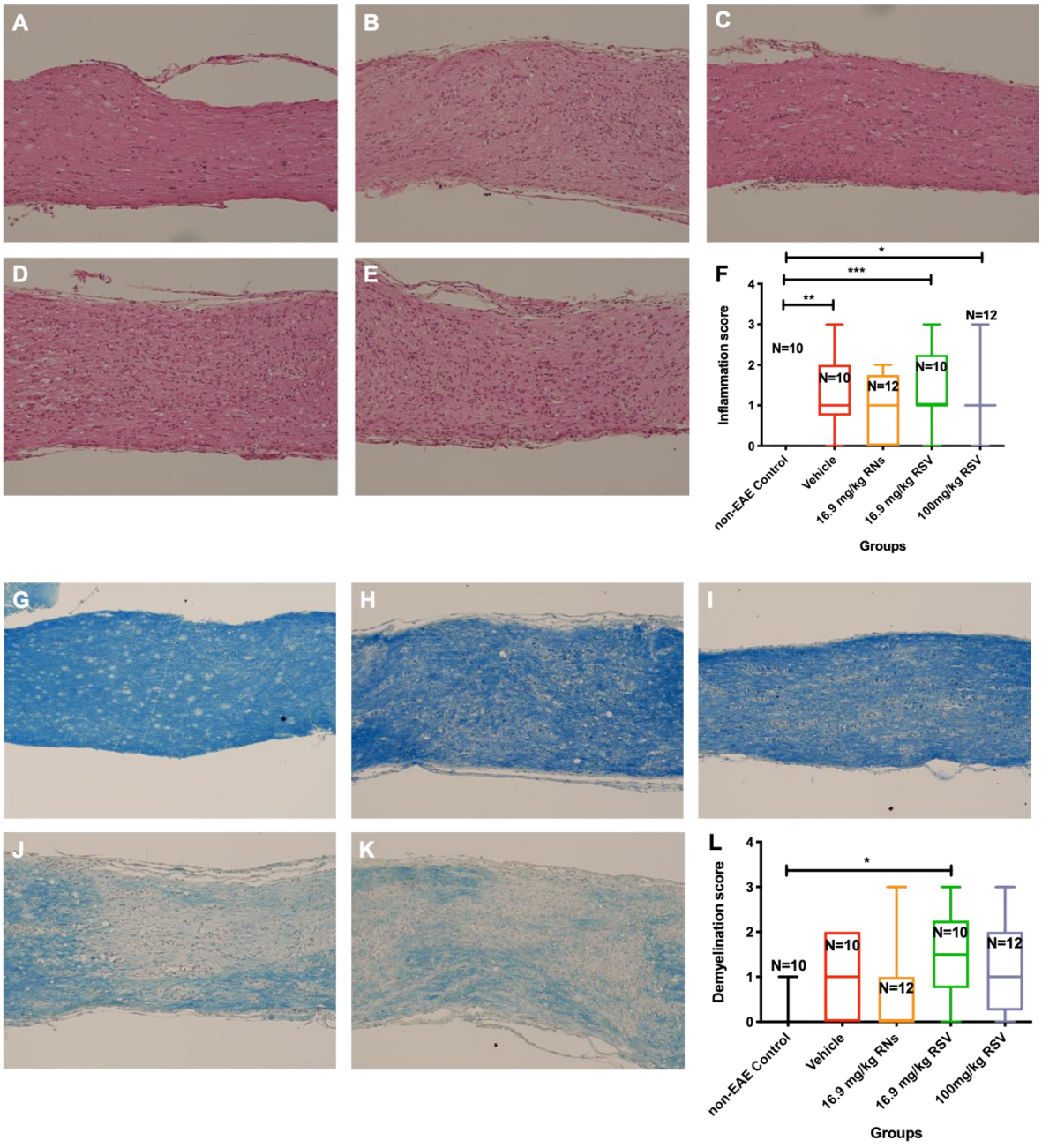

Figure 8. Optic nerve inflammation and demyelination after oral treatment with vehicle, RNs or RSV. H&E staining shows the cellularity and LFB the level of myelination in the optic nerve. Representative images of optic nerve longitudinal section inflammation in **(A)** non-EAE control, and EAE mice treated with **(B)** vehicle, **(C)** 16.9 mg/kg RNs, **(D)**16.9 mg/kg RSV and **(E)** 100 mg/kg RSV. **(F)** Optic nerve inflammation score was not significantly reduced with RN or RSV treatment. compared to the equivalent vehicle (Kruskal-Wallis with Dunn post-test, $p>0.05$). Non-EAE control did not show any optic nerve inflammation compared to significant inflammation in EAE mice (Kruskal-Wallis with Dunn post-test, *$p<0.05$, **$p<0.01$, ***$p<0.001$). Representative images of optic nerve longitudinal section demyelination in **(G)** non-EAE control, and EAE mice treated with **(H)** vehicle, **(I)** 16.9 mg/kg RNs, **(J)**16.9 mg/kg RSV and **(K)** 100 mg/kg RSV. **(L)** Optic nerve demyelination score was not significantly reduced with RN or RSV treatment compared to the equivalent vehicle (Kruskal-Wallis with Dunn post-test, $p>0.05$). 16.9 mg/kg RSV group had a significantly higher demyelination score than non-EAE control group (Kruskal-Wallis with Dunn post-test, *$p<0.05$). Images are original magnification x20.

Figure 8G-K shows representative LFB stained optic nerve sections used for demyelination assessment. Oral administration of 16.9 mg/kg RNs showed an important trend towards demyelination reduction without significance compared to vehicle (0.6 ± 0.3 vs 1.1 ± 0.3 demyelination score, p>0.05) while 16.9 mg/kg and 100 mg/kg RSV did not show any reduction compared to the vehicle (1.5 ± 0.3 and 1.2 ± 0.3 vs 1.1 ± 0.3 demyelination score, p>0.05) as shown in Figure 8L.

3.6 RNs show trend toward protection from visual decline

Visual function of EAE mice and non-EAE control mice was estimated by OKR before immunisation and once a week post-immunisation until sacrifice. EAE mice showed a progressive visual decline compared to the non-EAE control (Figure 9A). EAE mice treated with a daily oral administration of 16.9 mg/kg RNs had a slower decline than vehicle and other EAE treated mice. Thus, visual acuity (OKR) score was higher after treatment with 16.9 mg/kg RNs compared to vehicle, but the difference was not significant at day 28 (0.20 ± 0.04 vs 0.12 ± 0.04 OKR scores, p>0.05, Figure 9B).

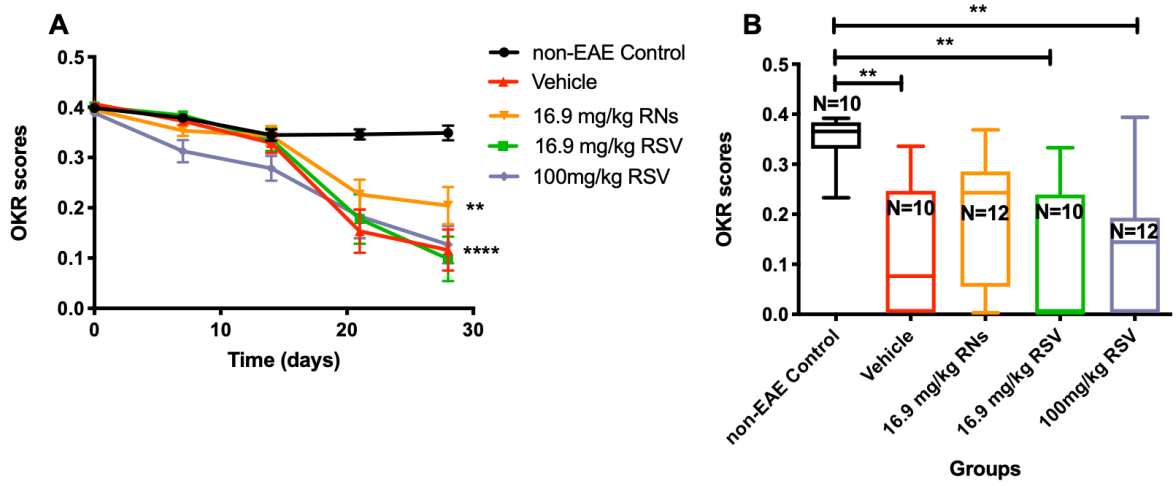

Figure 9. Visual function measured by OKR in non-EAE and EAE mice treated orally. (A) Visual function was reduced in EAE mice compared to non-EAE mice (two-way ANOVA of repeated measures with Tukey post-test, **p<0.01, ****p<0.0001), with a trend toward improved vision in EAE mice with 16.9 mg/kg RN as compared with EAE mice treated with vehicle, but this difference was not significant. **(B)** At day 28, OKR scores also showed a trend

toward being higher in 16.9 mg/kg RNs compared to vehicle treated EAE mice, but not significantly (one-way ANOVA with Tukey post-test, $p>0.05$). Non-EAE control mice had a higher OKR score than EAE mice treated with the vehicle, 16.9 mg/kg RSV or 100 mg/kg RSV (Kruskal-Wallis with Dunn post-test, $^{**}p<0.01$) but was not significantly different than EAE mice treated with 16.9 mg/kg RNs.

4. Discussion

The formulation of natural polyphenols with a good bioavailability and a simple manufacturing process is presently an unmet need. We provide results showing that 14.22 mg/ml resveratrol can be encapsulated in Solutol/TPGS with an EE over 70% and a stability over 3 months. Resveratrol encapsulated in Solutol/TPGS was also freeze-dried and stable with only a slightly reduced EE after rehydration. TPGS was chosen because of its ability to solubilise poor-water soluble molecules, inhibit P-glycoprotein and to increase drug bioavailability (15).

Spectroscopic techniques were used to determine the concentration of resveratrol in micellar formulations. Davis et al. have previously shown that there is a correlation between spectroscopic assessment and HPLC measures using curcumin encapsulated in Lutrol and TPGS (8). Overall, results demonstrate this resveratrol formulation achieves higher stability and/or concentrations than previously reported formulations (7).

Several groups have demonstrated that resveratrol can be formulated using natural and synthetic polymers, liposomes, micelles, SLN and silica nanoparticles (7). In one study, resveratrol loaded PLGA had a particle size of 202.8 ± 2.64 nm and an EE of 89.32 ± 3.51% with a concentration below 100 µg/ml (16). However, this study did not show any stability assessment. Wan et al. have also reported the formulation of resveratrol loaded PLGA nanoparticles at a concentration of 9 mg/ml and a stability of 2 months with an EE of 97.25%, a particle size of 176.1 nm and a PDI of 0.152 using

an emulsified solvent evaporation method (17). While these studies show promising results for the use of resveratrol as an oral treatment, the particle size obtained is much larger compared to our RNs (20 nm), limiting their utility for systemic administration. Studies have shown an inverted correlation between particle size and oral bioavailability. For example, retinoic acid formulations have demonstrated a 3-fold increase in oral bioavailability when the particle size decreased from 328.8 nm to 89.3 nm (18). Furthermore, the vast majority of these studies did not report the final concentration of resveratrol and did not show a long-lasting stability of resveratrol formulations (at least 3 months) as reported in this study. Our formulation stability correlates with Pandita et al. who also reported a stability of 3 months for their resveratrol SLN formulation when stored at 4°C (19), but their formulation is more complex to scale up and requires less biologically compatible solvents.

Resveratrol release from nanoparticles was highly reduced compared to resveratrol dissolved in 95% ethanol. The half-life $t_{1/2}$ of RNs was 76.86 h whereas it was 3.4 h for 14.22 mg/ml resveratrol dissolved in 95% ethanol demonstrating the sustained release capabilities of Solutol. Resveratrol formulation did not demonstrate an initial burst of resveratrol as less than 4% of drug was released after 6 hours, supporting the idea that resveratrol was not on the surface of the micelle but incorporated in the hydrophobic core as suggested by a previous study with resveratrol nanoparticles (20). In that study, X-ray diffraction on resveratrol nanoparticles showed the amorphous structure of resveratrol and its entrapment into the nanoparticles (20). In another study, PLGA only resveratrol nanoparticles had a release of 29% after 8 hours at pH 7.4 and 12.5% at pH 1.2 (17). This study did not assess the release in acidic condition which could be a mechanism to protect resveratrol from stomach acidity and increase its

absorption. The slow release of resveratrol from nanoparticles appears to be an important feature which might protect resveratrol from early metabolization and excretion, thus increasing its stability.

RNs given orally are able to prevent loss of RGCs, independent of any effect on reduction of inflammation in the optic nerve. Effects are similar to those reported previously using much higher doses of oral resveratrol formulations without use of nanoparticles (5). For example, chronic EAE mice treated with oral SRT501, a formulation of resveratrol, demonstrated a reduction of RGC loss compared to the control (2); however, 250 mg/kg of resveratrol given orally was able to delay the onset of neurological disabilities but not 100 mg/kg (2). These studies did not show a reduction of the inflammation in the spinal cord or the optic nerve, which is in agreement with our current results. Indeed, current results show oral administration of free resveratrol (100 mg/kg) requires five times higher concentrations compared to RNs (16.9 mg/kg) to induce neuroprotective effects, demonstrating a potential advantage of using this nanoparticle formulation instead of free resveratrol to treat disease. This suggests that our nanoparticles are able to increase the bioavailability of resveratrol. Indeed, the bioavailability of resveratrol following its encapsulation into different types of nanoparticles has been reported previously. For instance, Vijayakumar et al. reported that the intravenous administration in rats of SLN coated with TPGS containing resveratrol resulted in an 11 times higher area under the curve (AUC) and 9 times higher half-life than unconjugated resveratrol (21). Similarly, studies have shown an increase in resveratrol bioavailability and concentrations reaching the brain following the use of nanoparticles made of PLGA-TPGS (22) or galactosylated PLGA (23)

All of these studies suggest that resveratrol nanoformulations share an ability to increase resveratrol half-life and bioavailability. Although pharmacokinetic studies were not a focus of the current report, we demonstrated that RNs used in this research have properties consistent with increased bioavailability. RNs have a micellar structure protecting them from enzymatic degradation, increasing their absorption and slowing their release over time. They are also made of TPGS, a p-glycoprotein inhibitor.

Overall, findings suggest that resveratrol is able to reduce neuronal loss up to 30 days after immunisation whereas inflammation is not reduced. That might give room for immunomodulatory treatments to be used to treat inflammatory features of demyelinating disease in combination with RNs to prevent loss of neuronal cells. While not the focus of the current study aimed at improving bioavailability of resveratrol, previous reports have provided insight into how resveratrol may exert its effect without modulating inflammation. Studies have shown that SIRT1 activators like resveratrol promote mitochondrial function and reduce oxidative stress, leading to a reduction of neuronal loss in a viral-induced model of optic neuritis (24). Similarly, other studies have shown the increase of mitochondrial reactive oxygen species (25) and hydrogen peroxide (26) in EAE optic nerves 3 days after immunisation, before inflammation was detected, suggesting these are key features that may be targeted to reduce direct damage to neurons. Resveratrol likely exerts its neuroprotective effects through activation of the SIRT1 deacetylase, as studies have shown that inhibitors of SIRT1 led to an inhibition of resveratrol neuroprotective action in EAE (27). Interestingly, previous studies suggest resveratrol can reduce inflammation in some neurologic injury models by inhibiting NF-κB signalling pathway (28) or directly inhibiting the

secretion of proinflammatory cytokines including interleukine (IL)-6, IL-8, and Tumor necrosis factor (TNF)-α (29). Similarly, resveratrol promoted remyelination in a cuprizole model of MS (30), albeit when given at a higher dose of 250 mg/kg. However, several studies in the EAE model consistently found that resveratrol, and other treatments that upregulate SIRT1, selectively prevent neuronal loss without significantly reducing inflammation (2,27,31-33), suggesting that inflammatory responses in EAE may be less susceptible to resveratrol. The ability of resveratrol, and RNs in the current study, to prevent RGC loss independent of ongoing inflammation may provide a key clinical adjunct to current corticosteroid and immunomodulatory therapies that speed recovery times in acute optic neuritis but fail to prevent RGC loss and its associated permanent visual dysfunction. Results suggest RNs warrant further evaluation as potential combination therapy with corticosteroids for treatment of optic neuritis.

5. Conclusions

This study has shown that resveratrol can be formulated into a stable formulation which increases its bioavailability with improved size and stability compared with prior reported resveratrol nanoparticle formulations. Importantly, these improved RNs demonstrate potential clinical utility by promoting neuroprotective effects on RGC survival in an EAE model of demyelinating disease. Results support the use of nanoparticle formulation of resveratrol in other disease models involving neurodegeneration. Further studies are needed to confirm these results.

6. References

1. McGinley MP, Goldschmidt CH, Rae-Grant AD. Diagnosis and Treatment of Multiple Sclerosis: A Review. JAMA. 2021 Feb 23;325(8):765–79.
2. Fonseca-Kelly Z, Nassrallah M, Uribe J, Khan RS, Dine K, Dutt M, et al. Resveratrol Neuroprotection in a Chronic Mouse Model of Multiple Sclerosis. Front Neurol. 2012;3:84.
3. Berman AY, Motechin RA, Wiesenfeld MY, Holz MK. The therapeutic potential of resveratrol: a review of clinical trials. npj Precis Oncol 2017 11. 2017 Sep 25;1(1):1–9.
4. Abu-Amero K, Kondkar A, Chalam K. Resveratrol and Ophthalmic Diseases. Nutrients. 2016 Apr 5;8(4):200.
5. Drygalski K, Fereniec E, Koryciński K, Chomentowski A, Kiełczewska A, Odrzygóźdź C, et al. Resveratrol and Alzheimer's disease. From molecular pathophysiology to clinical trials. Exp Gerontol. 2018 Nov 1;113:36–47.
6. Crowell JA, Korytko PJ, Morrissey RL, Booth TD, Levine BS. Resveratrol-Associated Renal Toxicity. Toxicol Sci. 2004 Dec 1;82(2):614–9.
7. Ahmadi Z, Mohammadinejad R, Ashrafizadeh M. Drug delivery systems for resveratrol, a non-flavonoid polyphenol: Emerging evidence in last decades. J Drug Deliv Sci Technol. 2019 Jun 1;51:591–604.
8. Davis BM, Pahlitzsch M, Guo L, Balendra S, Shah P, Ravindran N, et al. Topical Curcumin Nanocarriers are Neuroprotective in Eye Disease. Sci Rep. 2018;8(1):11066.
9. Strickley RG. Solubilizing Excipients in Oral and Injectable Formulations. Vol. 21, Pharmaceutical Research. Springer; 2004. p. 201–30.
10. Davis BM, Normando EM, Guo L, Turner LA, Nizari S, O'Shea P, et al. Topical delivery of Avastin to the posterior segment of the eye in vivo using annexin A5-associated liposomes. Small. 2014 Apr;10(8):1575–84.
11. A basic introduction to Dynamic Light Scattering (DLS) for particle size analysis | Malvern Panalytical [Internet]. [cited 2020 Dec 29]. Available from: https://www.malvernpanalytical.com/en/learn/events-and-training/webinars/W180201BasicDynamicLightScattering
12. Khan RS, Dine K, Bauman B, Lorentsen M, Lin L, Brown H, et al. Intranasal Delivery of A Novel Amnion Cell Secretome Prevents Neuronal Damage and Preserves Function In A Mouse Multiple Sclerosis Model. Sci Rep. 2017;7:41768.
13. Willett K, Khan RS, Dine K, Wessel H, Kirshner ZZ, Sauer JL, et al. Neuroprotection mediated by ST266 requires full complement of proteins secreted by amnion-derived multipotent progenitor cells. PLoS One. 2021 Jan 1;16(1):e0243862.
14. Khan RS, Ross AG, Willett K, Dine K, Banas R, Brown LR, et al. Amnion-Derived Multipotent Progenitor Cells Suppress Experimental Optic Neuritis and Myelitis. Neurother 2020 181. 2020 Oct 16;18(1):448–59.
15. Guo Y, Luo J, Tan S, Otieno BO, Zhang Z. The applications of Vitamin e TPGS in drug delivery. Vol. 49, European Journal of Pharmaceutical Sciences. Elsevier; 2013. p. 175–86.
16. Nassir AM, Shahzad N, Ibrahim IAA, Ahmad I, Md S, Ain MR. Resveratrol-loaded PLGA nanoparticles mediated programmed cell death in prostate cancer cells. Saudi Pharm J. 2018 Sep 1;26(6):876–85.

17. Wan S, Zhang L, Quan Y, Wei K. Resveratrol-loaded PLGA nanoparticles: enhanced stability, solubility and bioactivity of resveratrol for non-alcoholic fatty liver disease therapy. R Soc Open Sci. 2018 Nov 30;5(11):181457.
18. Wang Y, Pi C, Feng X, Hou Y, Zhao L, Wei Y. The Influence of Nanoparticle Properties on Oral Bioavailability of Drugs . Int J Nanomedicine. 2020 Aug 24;15:6295–310.
19. Pandita D, Kumar S, Poonia N, Lather V. Solid lipid nanoparticles enhance oral bioavailability of resveratrol, a natural polyphenol. Food Res Int. 2014 Aug 1;62:1165–74.
20. Kamath MS, Ahmed SSSJ, Dhanasekaran M, Winkins Santosh S. Polycaprolactone scaffold engineered for sustained release of resveratrol: Therapeutic enhancement in bone tissue engineering. Int J Nanomedicine. 2013 Dec 23;9(1):183–95.
21. Vijayakumar MR, Kumari L, Patel KK, Vuddanda PR, Vajanthri KY, Mahto SK, et al. Intravenous administration of: Trans -resveratrol-loaded TPGS-coated solid lipid nanoparticles for prolonged systemic circulation, passive brain targeting and improved in vitro cytotoxicity against C6 glioma cell lines. RSC Adv. 2016 May 18;6(55):50336–48.
22. Vijayakumar MR, Kosuru R, Singh SK, Prasad CB, Narayan G, Muthu MS, et al. Resveratrol loaded PLGA:D-α-tocopheryl polyethylene glycol 1000 succinate blend nanoparticles for brain cancer therapy. RSC Adv. 2016 Aug 3;6(78):74254–68.
23. Siu F, Ye S, Lin H, Li S. Galactosylated PLGA nanoparticles for the oral delivery of resveratrol: enhanced bioavailability and in vitro anti-inflammatory activity. Int J Nanomedicine. 2018 Jul;Volume 13:4133–44.
24. Khan RS, Dine K, Das Sarma J, Shindler KS. SIRT1 Activating compounds reduce oxidative stress mediated neuronal loss in viral induced CNS demyelinating disease. Acta Neuropathol Commun. 2014 Jan 27;2(1):3.
25. Qi X, Lewin AS, Sun L, Hauswirth WW, Guy J. Suppression of mitochondrial oxidative stress provides long-term neuroprotection in experimental optic neuritis. Investig Ophthalmol Vis Sci. 2007 Feb 1;48(2):681–91.
26. Guy J, Ellis A, Mames R, Rao NA. Role of Hydrogen Peroxide in Experimental Optic Neuritis. Ophthalmic Res. 1993;25(4):253–64.
27. Shindler KS, Ventura E, Dutt M, Elliott P, Fitzgerald DC, Rostami A. Oral resveratrol reduces neuronal damage in a model of multiple sclerosis. J Neuro-Ophthalmology. 2010 Dec;30(4):328–39.
28. Xu L, Botchway BOA, Zhang S, Zhou J, Liu X. Inhibition of NF-κB Signaling Pathway by Resveratrol Improves Spinal Cord Injury. Front Neurosci. 2018 Oct 4;12(OCT):690.
29. Latruffe N, Lançon A, Frazzi R, Aires V, Delmas D, Michaille JJ, et al. Exploring new ways of regulation by resveratrol involving miRNAs, with emphasis on inflammation. Ann N Y Acad Sci. 2015;1348(1):97–106.
30. Ghaiad HR, Nooh MM, El-Sawalhi MM, Shaheen AA. Resveratrol Promotes Remyelination in Cuprizone Model of Multiple Sclerosis: Biochemical and Histological Study. Mol Neurobiol. 2017 Jul 1;54(5):3219–29.
31. Shindler KS, Ventura E, Rex, TS, Elliott P, Rostami A. SIRT1 Activation Confers Neuroprotection in Experimental Optic Neuritis. Invest Ophthalmol Vis Sci. 2007;48(8):3602-9.
32. McDougald DS, Dine KE, Zezulin AU, Bennett J, Shindler KS. SIRT1 and NRF2 Gene Transfer Mediate Distinct Neuroprotective Effects Upon Retinal Ganglion Cell Survival

and Function in Experimental Optic Neuritis. Invest Ophthalmol Vis Sci. 2018;59:1212-20.
33. Ross AG, Chaqour B, McDougald DS, Dine KE, Duong TT, Shindler RE, Yue J, Liu T, Shindler KS. Selective Upregulation of SIRT1 Expression in Retinal Ganglion Cells by AAV-Mediated Gene Delivery Increases Neuronal Cell Survival and Alleviates Axon Demyelination Associated with Optic Neuritis. Biomolecules 2022;12:830.